

Interim Progress Report for CDFR Agreement Number 15-0214SA

GENOME EDITING OF *TAS4*, *MIR828* AND TARGETS *MYBA6/A7*: A CRITICAL TEST OF *XYLELLA FASTIDIOSA* INFECTION AND SPREADING MECHANISMS IN PIERCE'S DISEASE

Principal Investigator:

Chris Rock
Texas Tech University
Dept of Biological Sciences
Lubbock, TX 79409-3131
chris.rock@ttu.edu

Cooperator:

Leo De La Fuente
Auburn University
Dept Entomology Plant Pathology,
Auburn, AL 36849
lzd0005@auburn.edu

Cooperator:

David Tricoli
University of California, Davis
Plant Transformation Facility
Davis, CA 95616
dmtricoli@ucdavis.edu

Research Associate:

Sunitha Sukumaran
Texas Tech University
Dept of Biological Sciences
Lubbock, TX 79409-3131
sunitha.sukumaran@ttu.edu

Graduate Research Asst:

Md. Fakhrul Azad
Texas Tech University
Dept of Biological Sciences
Lubbock, TX 79409-3131
fakhrul.azad@ttu.edu

Research Associate:

Sy Mamadou Traore
Auburn University
Dept Entomology Plant Pathology,
Auburn, AL 36849
traorsm@auburn.edu

Reporting Period: The results reported here are for work conducted from Oct 12, 2016- Feb. 28, 2017.

INTRODUCTION

Our working model of PD etiology postulates microRNA828 (miR828) and evolutionarily-related *Trans-Acting Small-interfering locus4 (TAS4)* activities silence target *VvMYBA6/A7* and other homologous *MYB* targets' expression in response to *Xylella fastidiosa* (XF) infection, mediated through inorganic phosphate (P_i) known in other species to regulate miR828 and other miRNA expressions^{1,2}. New deep sequencing transcriptome- and small RNA-Seq data are in hand and being analyzed genome-wide to consider other phosphate-regulated miRNAs as additional nodes in a network of miRNA and phased, small-interfering RNA (phasiRNA) effectors of PD etiology, driven by results to date and presented at the 2016 PD-GWSS Symposium. We are currently testing the XF infection/spread-via-host-miRNA-derangement hypothesis directly by "knocking out" the key hypothesized *MIR828/TAS4/MYB* genes using a new genome editing technology- Clustered Regularly Interspaced Short Palindromic Repeats (CRISPR/Cas9)^{3,4} that the CDFR-PD Board nominated as a feasible, high-priority approach to engineering PD resistance.

We are also taking a complimentary "overexpression" approach in tobacco to directly test the MYB-anthocyanins-as-XF-effectors hypothesis. The surrogate tobacco XF infection system developed by the Cooperator (De La Fuente)⁵ can quickly assess susceptibility to XF infection of a transgenic tobacco line⁶ (Myb237) that over-expresses the Arabidopsis orthologue of *VvMYBA6/A7: PRODUCTION OF ANTHOCYANIN PIGMENT2/MYB90*. We have repeated the greenhouse XF challenge experiment on MYB overexpression genotypes and report here our findings to date. Results of the first test were reported previously (Feb., 2016) in support of the working hypothesis.

With successful production by the Cooperator (Tricoli, see below) of transgenic tobacco plants expressing the *MIR828/TAS4/MYB* CRISPR/Cas9 vectors, another tool will become available to characterize editing activity on endogenous Nt-*MIR828/TAS4/MYB* targets of our CRISPR vectors in a heterologous system, while grapevine transgenic regeneration proceeds.

OBJECTIVES (as funded)

- I. Demonstrate the efficacy of CRISPR/Cas9 transgenic technology for creating deletion mutants in *MIR828*, *TAS4*, and target *MYBA6/7*. When validated, future experiments will critically test these genes' functions in PD etiology and XF infection and spreading.
- II. Characterize tissue-specific expression patterns of *TAS4* and *MIR828* primary transcripts, sRNAs, and *MYB* targets in response to XF infections in the field, and in the greenhouse for tobacco transgenic plants overexpressing *TAS4* target gene *AtMYB90/PRODUCTION OF ANTHOCYANIN PIGMENT2*.
- III. Characterize the changes in (a) xylem sap and leaf inorganic phosphate (Pi), and (b) polyphenolic levels of XF-infected canes and leaves. (c) Test on tobacco in the greenhouse and XF growth *in vitro* the Pi analogue phosphite as a durable, affordable and environmentally sound protectant/safener for PD.

DESCRIPTION OF ACTIVITIES CONDUCTED TO ACCOMPLISH OBJECTIVES

I. Test the miR828, *TAS4*, and target *MYBA6/7* functions in PD etiology and XF infection and spreading by genome editing using CRISPR/Cas9 transgenic technology

Engineered binary T-DNA *Agrobacterium* vectors designed to genome edit the grapevine *VvMIR828*, *VvTAS4ab*, and target *VvMYBA6/VvMYBA7* loci (described in Oct. 2015 progress report) were electroporated by the PI into EHA105 obtained from Stan Gelvin, Purdue University, and sent to the Collaborator David Tricoli's lab under APHIS BRS permit # 15-231-102m in Nov., 2015. Three independent transformation cycles for each construct were initiated in November-December 2015, and May 2016. Problems associated with both Thompson seedless and rootstock 101-14 transformation/regeneration were described in the July 2016 progress report, and confirmed by using the same Agro vector strains to transform tobacco, reported in Oct 2016. We presented molecular evidence (Southern blot of restriction digests of the vectors propagated in both *E. coli* and *Agrobacterium tumefaciens*) at the 2016 PD- GWSS Symposium that the vectors were not the problem. The PI then obtained the EHA105 *A. tumefaciens* strain from the Cooperator (Tricoli) and now the problem (starting strain, apparently) has been solved. **Fig. 1** shows good transformation efficiency of the CRISPR vectors delivered by the EHA105 *A. tumefaciens* stock EHA105 used routinely by the Cooperator. Based on these results



Fig. 1. Tobacco transformation test of p201-N-Cas9 vectors (Addgene#59175; middle right) in Cooperator-sourced EHA105 Agro strain and derivative constructs, showing good response. Positive control (lower right) used the same EHA105 *A. tumefaciens* strain and a Kan^R vector routinely in use in the Tricoli lab.

verifying the vector activity, two sets of of grapevine somatic embryo transformation of rootstock 101-14 were initiated on 2/8/2017 and 2/15/2017. Two more sets of experiments on rootstock '1103-P' will begin soon and regenerated plants are anticipated to be received in Oct 2017.

Validation of editing events and characterization of editing efficiencies going forward will be performed on these resultant transgenic tobacco and future regenerated grapevines by PCR cloning and sequencing of target genes, and PAGE-based genotyping⁷. We have mined the draft tobacco genomes (<https://solgenomics.net/tools/blast/>) and obtained evidence that several of our synthetic guide vectors targeting grapevine candidate effectors (documented in Mar. 2016 progress report) should function to target the endogenous tobacco *Nt-MIR828a* and both *Nt-TAS4a,-b*. This claim is based on the essential requirement of

Streptococcus pyogenes nuclease Cas9 for a perfect guide match to the 'seed' region (nucleotides 1-5, less essential in nt 7-12)⁸. The Vv-MIR828* guide has a mismatch at guide seed position 9 of Nt-MIR828a. The Vv-TAS4a guide that targets the functional tasi-RNA 3'D4(-) species has a mismatch at nt 11 to both Nt-TAS4a and -TAS4b (data not shown). Thus, although candidate target Nt-MYBs (there are three; data not shown) are not expected to be targeted by the Vv-MYBA6/7 synthetic guide RNAs, the transgenic tobacco materials forthcoming in the next couple of months will be fertile ground to test activity of our CRISPR/Cas9 vectors *in planta*. We reported in Oct. 2016 progress report an established deletion detection PAGE assay in our lab using a known 15 nt deletion of the phytochrome *PHYD-1* gene of Arabidopsis ecotype Wassilewskija (Ws-2)⁹. If target editing of the tobacco MIR828 and/or TAS4 loci is validated, then the transgenic plants can be challenged with XF like has been done in AtMYB90 overexpressing tobacco as a direct test of the working hypothesis that *MIR828/TAS4/MYB* effectors are necessary for PD etiology.

Summary of accomplishments and results, Objective I. A technical issue that delayed progress of grapevine transformation has been solved, and as a fringe benefit a new tool (transgenic tobacco) to study the role of *MIR828/TAS4/MYB* genes in PD developed. We are on track to complete the production of deliverable transgenic grapevines and characterize novel transgenic tobacco plants this calendar year.

II. Characterize tissue-specific expression patterns of *TAS4* and *MIR828* primary transcripts, siRNAs, and *MYB* targets in response to XF infections in the field, and in the greenhouse for tobacco transgenic plants overexpressing *TAS4* target gene *AtMYB90/PRODUCTION OF ANTHOCYANIN PIGMENT2*.

In the previous progress reports and the 2016 PD-GWSS Symposium we characterized and correlated molecular phenotypes of XF titres, TAS4-3'D4(-) siRNA and miR828 abundances by RNA blot estimation, and anthocyanin quantities extracted from the transgenic tobacco line Myb237 overexpressing AtMYB90 challenged with XF in the greenhouse, and from PD-infected and symptomless Merlot leaves and petioles collected from the 'Calle Contento' vineyard in Temecula CA, and the Black Stock vineyard in Dahlonga, Lumpkin Co., GA. Those compelling results and preliminary analyses of our first and second Illumina small RNA (and transcriptome, for grape) libraries generated from the same tobacco- and California XF-infected and control samples strongly support the working model of XF interaction with anthocyanin biosynthesis regulation by the host during PD progression. Results showed significant differences in accumulation of anthocyanins in XF-infected vs. control leaves from the field and greenhouse samples. Cooperators De La Fuente and Traore repeated the tobacco Myb237 XF challenge experiment and preliminary analyses of the repeat experiment support the previous observation of significantly greater (~50% of leaves) disease symptom development in homozygous (Hmo) MYB overexpressing lines five weeks after XF challenge. **Table I** shows the results of anthocyanin quantitation of the repeat greenhouse experiment, compared to results from 2015.

Table I. Quantitation from repeat experiments of anthocyanins in transgenic tobacco genotypes challenged in the greenhouse with or without XF.			
Sample	µmoles cyanidin-O-Glu/mg fw equivalents (± s.e.m.)		Week 5, Disease incidence index
	2016 experiment†	2015 experiment*	
tobacco SR1, XF-infect	0.54 (± 0.09)	0.7 (± 0.2)	+
tobacco SR1, buffer	0.56 (± 0.11)	0.7 (± 0.4)	N.D.
MYB90-OX Hmi, XF-inf	1.07¶ (± 0.18)	7.8 (± 0.4)	+
MYB90-OX Hmi, buffer	1.86 (± 0.24)	2.0 (± 0.9)	N.D.
MYB90-OX Hmo, XF-inf	2.34¶ (± 0.11)	3.4 (± 0.5)	++
MYB90-OX Hmo, buffer	3.52 (± 0.15)	2.7 (± 0.1)	N.D.

* Three biological replicates. † Five biological replicates. N.D. not detected
 + indicates ~25% of leaves show scorching; ++ indicates ~50% leaf scorching.
 ¶ significantly different than buffer control, *P* < 0.05

We are in process of quantifying XF titres to correlate with disease severity, which was again observed greater in the homozygous (HMO) transgenics compared to heterozygous or control genotypes (**Fig. 2**). In the 2016 repeat experiment there is a trend toward XF infection causing a significant decrease in anthocyanins, consistent with the model; it remains to be seen if this will be corroborated at the molecular level in these new tobacco samples of predicted increases in negative effectors of anthocyanins miR828/TAS4 siRNAs, and

decreased expression of target *MYB* mRNAs. This is the opposite direction (i.e. anthocyanin accumulation; data not shown) for PD symptoms in grapevine leaves. Systems analyses show significantly different, and most importantly, inverse changes of mRNA and siRNA expressions for secondary metabolism genes in XF-infected 2015 field samples from 'Calle Contento' Temecula vineyard compared to controls. **Fig. 3** shows a cogent example of results to date for an inverse correlation¹⁰ of abundances of phased, small interfering RNAs (phasiRNAs) **significantly down-regulated** by XF infection (4th column of bar grid) and mapping to cognate **mRNA targets significantly up** (1st column bars) in ontology bins for secondary metabolism, specifically flavonoids/flavonols and anthocyanins in response to XF infection. This inverse relationship is speculated to be functionally significant, whereby secondary (polyphenolics) metabolism is impacted by upstream hierarchical activation of negative regulators miR828 and *TAS4* siRNAs, which results in altered (decreased) phasiRNAs and up-regulation of mRNA templates of the phasiRNAs.

A major consideration for the observed difference in anthocyanin changes between XF-infected tobacco and grape, besides the non-endogenous transgene expression of positive anthocyanin effector in the tobacco experiment, is that the timing of sampling after infection varied between the greenhouse (5 weeks) and field samples (endemic infection, months-old leaves). There is evidence that early host responses to XF infection are up-regulation of resistance effector genes like *PdR1* candidate *VIT_14s0171g00180* (Andy Walker, pers. comm.), followed late in infection by strong down-regulation (**Fig. 4**; Mapman¹¹ data not shown).

We previously reported (Oct. 2016 report) strong evidence, based on sRNA blots and normalized deep sequencing read counts that XF infection triggers up regulation of miR828 and *TAS4* siRNAs in field samples from CA used for construction of deep sequencing libraries. We also previously described results showing in non-transgenic control tobacco plants XF induces *TAS4* siRNA production triggered by miR828, albeit at 1000x lower levels than in *AtMY90*-overexpressing tobacco. Those data strongly support our working model for PD etiology mediated by miR828 induction. Furthermore, we have obtained conclusive evidence for deep evolutionary conservation of the autoregulatory loop we documented in *Arabidopsis*¹²: *AtMYB90/PAP2* (a *TAS4* target) functions as a positive regulator of endogenous *Nt-TAS4* and *Nt-MIR828* expression and remarkably, XF infection suppresses this effect (**Fig. 5**). It remains unclear at what level XF acts in the autoregulatory loop, or possibly higher up in a hierarchy of transcription factors, because interpretation is confounded by autoregulatory activity of either *PAP2* or endogenous cognate *MYBs*.

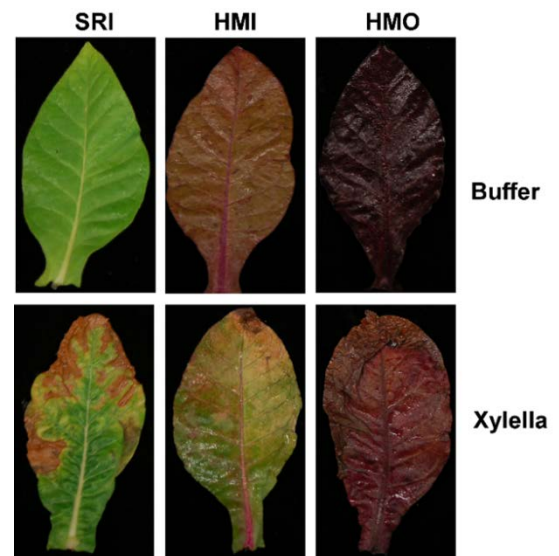


Fig. 2. 2016 repeat experiment of XF challenge of tobacco over-expressing *TAS4* target *AtMyb90/PAP2*. Results corroborate that homozygous genotype (HMO) infected with XF has more severe symptoms than heterozygous (HMI) or control (SRI).

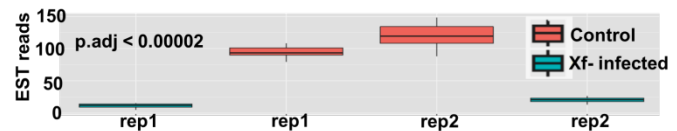


Fig. 4. Significant down regulation by XF infection of *PdR1* candidate Leucine-Rich Repeat receptor revealed by mRNA-Seq of 2015 field samples from 'Calle Contento' vineyard, Temecula CA.

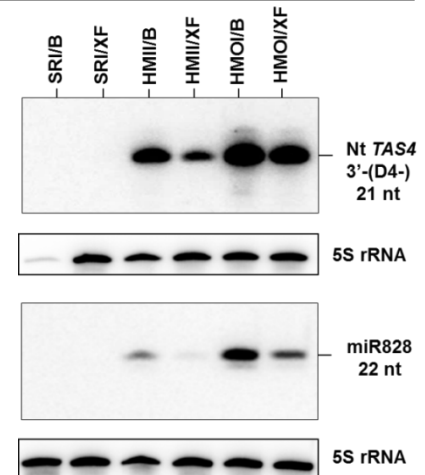


Fig. 5. Evidence for deep conservation of the *TAS4* autoregulatory loop: *PAP2* (*AtMYB90*, *TAS4* target) overexpression in tobacco line *Myb237* induces the endogenous *Nt-TAS4-3'D4(-)* and its trigger *Nt-miR828*, and XF infection changes the autoregulatory loop dynamic.

We have made Illumina TruSeq stranded degradome libraries^{13, 14} for discovery of the sRNA triggers of transitivity revealed by ShortStack¹⁵ and PhaseTank¹⁶ softwares and are in process of compiling the results. This systems approach builds on the identified sRNA candidates and importantly will uncover genome-wide leads for other etiological effectors/reporters of PD and network analyses of gene interactions affecting primary and

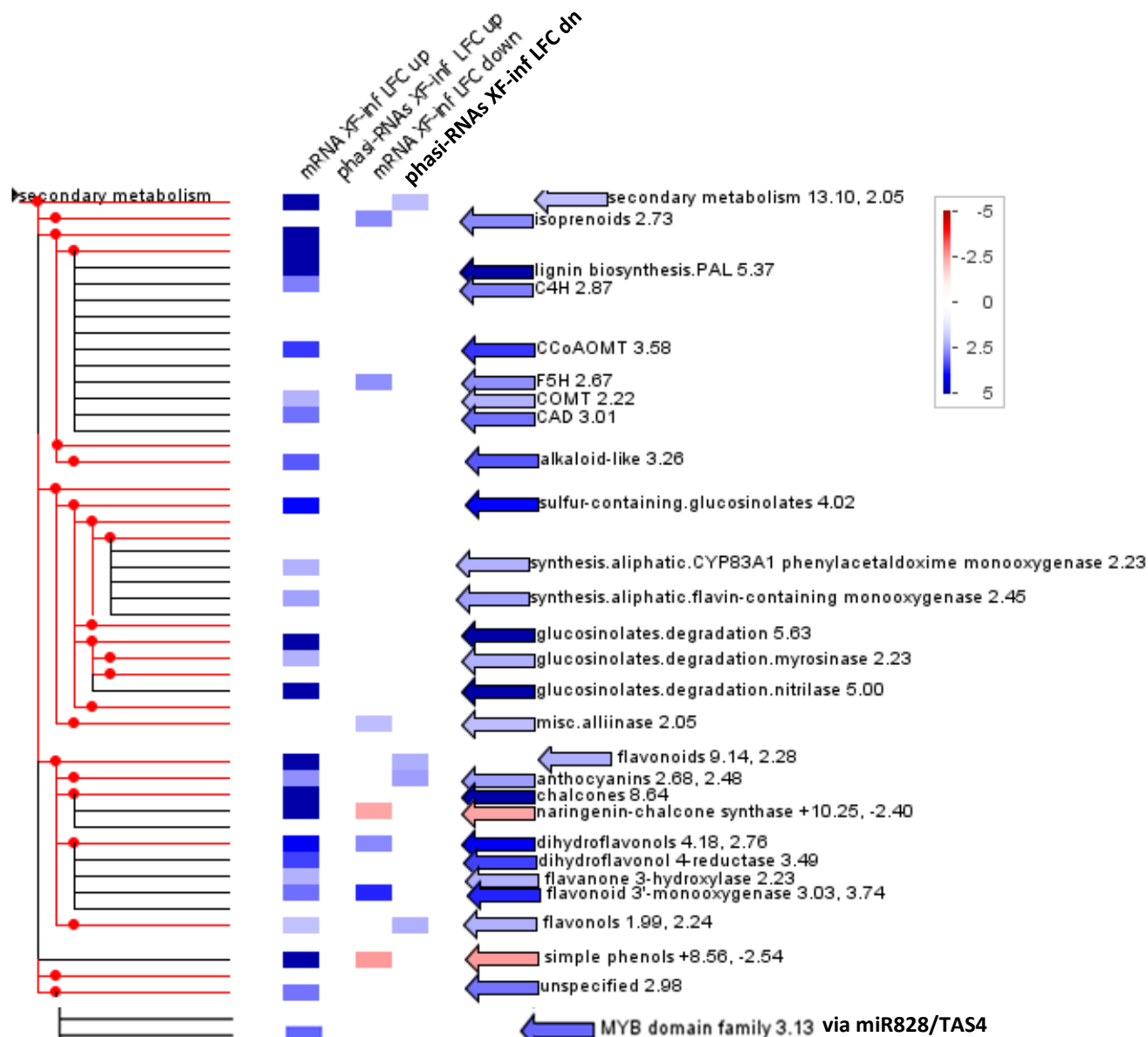


Fig. 3. Fisher Exact Test (Mapman software) for fold over- (blue) and under-representation (red) of significantly differentially expressed (DE, both up- and down-) genes of phenylpropanoid and positive effector MYB transcription factors known by functional studies and phylogeny from other species to control the biosynthetic pathway. Clusters spanning RNA-Seq and sRNA-Seq libraries very strongly support the working model that XF infection results in compelling DE of mRNAs AND their derived phasiRNAs for these ontology bins associated with PD. There are many leads revealed (data not shown) for miRNA/tasiRNA networks from this analysis, in addition to evidence for causal role of TAS4/miR828 in up-regulation of MYB effectors of phenylpropanoid biosynthesis.

secondary metabolism and disease resistance mechanisms. **Table II** shows preliminary quantitative and qualitative analyses by ShortStack and PhaseTank softwares, respectively, for endogenous Nt-miR828 and Nt-TAS4 phasi-RNA production and prediction of a novel *TAS* (*PHAS_SS11671*) with evidence from the degradome libraries that miR828 triggers phasiRNAs predicted to target mRNAs. Direct demonstration of altered expression by XF of the causal effector (miR828) for regulatory cascades is a significant advance that strengthens our claims,

in lieu of deep sequencing proofs which should be forthcoming when the degradome data analyses are finished and the regulatory cascade topology elucidated by systems approaches. We have identified many novel miRNAs and a few of their candidate *TAS* targets as a 'blue skies' by-product of our deep sRNA and degradome datasets.

Table II. Normalized miR828 and *TAS4* expression in heterozygous (HMI) and homozygous (HMO) transgenic tobacco overexpressing *TAS4* target AtMYB90, with or without XF infection for five weeks. Numbers in **bold** are evidence that Xylella induces *MIR828* and *TAS4* expression. Lower normalized reads (*italics*) in HMO genotype in response to XF support findings by small RNA blot analysis (Fig. 5) that XF negatively affects MYB90→*TAS* autoregulation activity.

	Genotype/treatment											
	control						infected					
	SR1		HMI		HMO		SR1		HMI		HMO	
Experiment year	'15	'16	'15	'16	'15	'16	'15	'16	'15	'16	'15	'16
Locus_TN90contig#	small RNA reads per 10M											
Nt- <i>MIR828a</i> _SS16401	0	0	0	0	0	5.0	0	0	0	0.4	0	2.3
Nt- <i>MIR828b</i> _SS15506	0	0	4.9	2.4	3.5	11.2	0	0.3	3.0	2.4	1.7	7.8
Nt- <i>TAS4a</i> _SS16012*	0	6.3	8488	3694	7878	16406	6.2	26.9	9356	3312	3544	8120
Nt- <i>TAS4b</i> _SS10361	0	14.3	16968	4113	12589	33246	2.5	46.6	14713	5279	7421	16723
<i>PHAS</i> _SS11671_828trigger [†]	0	0	0	0.9	0	0	0	0.3	3.0	3.2	0	0

**TAS4a* phase score 52.6. [†]Phase score 34.7; identified a miR828-triggered novel *TAS* locus by PhaseTank [16].

We have found additional compelling evidence in the literature supporting our phosphate-regulation XF etiology model: in Arabidopsis infected with XF, genome-wide transcriptome analysis showed *TAS4* siRNA target *MYB PRODUCTION OF ANTHOCYANIN PIGMENT1/MYB75* and another phosphate-regulated locus, At5g20150/SPX DOMAIN, which is a positive regulator of cellular responses to phosphate starvation, are both strongly down regulated by XF infection¹⁷. Furthermore, SPX1 messenger RNA is mobile in the vasculature¹⁸, which is relevant to the XF growth habitat. These serendipitous findings constitute 'smoking guns' supporting our working model and raise the possibility that other sRNA and/or pathogenesis regulons are also involved. The ongoing analyses of the mRNA, sRNA, and degradome deep sequencing datasets from multiple replicate libraries made from the 2015 and 2016 Temecula CA vineyard samples are expected further substantiate our findings and leverage 'blue skies' discoveries of regulatory networks of *PHAS*, *TAS*, and miRNA effectors of PD.

We are currently analyzing the mRNA-Seq, sRNA, and degradome datasets with the statistical software DESeq2¹⁹ for computational identification of differentially expressed clusters of small RNA-producing loci mined with ShortStack and PhaseTank from the 2015 and 2016 XF-infected and control Temecula CA libraries. **Table III** shows a short list of top leads that are significantly differentially expressed in XF-infected leaves. Although low base mean read depths for *MIR828*, *TAS4abc*, and those MYB targets of miR828²⁰ and *TAS4*-3'D4(-) (*MYBA6/A7*) that produce phased siRNAs²¹ precludes conclusive evidence for their *significantly* different expressions in response to XF to date, the trend is very clear and compelling- XF infection in all cases results in a several-fold up regulation of transitivity inferred to be triggered by miR828 (shown for grape XF samples by RNAblot) and/or *TAS4*-3'D4(-). Based on strong correlations seen across other libraries previously analyzed²¹, *Vv-TAS4c* is emerging as the likely causal effector for XF response. The diversity and conservation of phasiRNA loci across plant taxa²²⁻²⁵ revealed thus far by our results encompasses orthologues of *MYB-L3* triggered by miR828 in many species²⁶⁻³⁴, including grape²⁰; *TAS* effectors *SUPPRESSOR OF GENE SILENCING3 (SGS3)* and *DCL2*^{30, 35} (Table III), and the huge families of *LRR* and *PPRs* targeted by ancient, homologous miRNAs 472/482/2118^{24, 26, 30} and *TAS1-3/miR390/ 4376/7122*^{34, 36}, respectively. Their collective loss in virus- and bacteria-infected tissues that results in susceptibility^{24, 37} supports their functions as master regulators targeted by XF, and possibly Grapevine Red Blotch-associated Virus.

Regarding the role of phosphate signaling in our working model, we note two studies previously documented mis-regulation of *SPX1* in response to 8 weeks XF incubation in grapevine³⁸ and at 9 days post XF

infection in Arabidopsis¹⁷. *NITROGEN LIMITATION ADAPTATION* and close homologues in Arabidopsis and monocots are known to encode SPX-RING-finger-type ubiquitin E3 ligases targeted by miR827^{1, 39-42} that function in phosphate signaling in conjunction with miR399-targeted E2 conjugase *PHO2*, to direct 26S proteasome ubiquitin-mediated degradation of a family of membrane-localized Major Facilitator Superfamily (MFS) phosphate translocators alternatively called PHTs^{42, 43}. Grapevine phosphate transporter *VvPHT2;1* was shown previously to be significantly down-regulated eight weeks after XF infection³⁸. We observe the same down-regulation of *PHT2;1* in our XF data (Table III). Hailing Jin previously showed the citrus homologue of

Table III. XF infection effects on expression of phasiRNAs (sRNA-Seq) mapping to mRNAs (mRNA-Seq) from CA Temecula samples (July 2015). Green boxes show up-regulated phasiRNAs and miRNA effectors; red boxes show the inverse correlation of target mRNA abundance, supporting hypothesized gene silencing triggered by miRNAs.

Annotation	phas-score*	Control*	XF infected*	phasiRNA L ₂ FC [‡]	phasi p-val	mRNA L ₂ FC [†]	mRNA q-val [¶]
Vv- <i>TAS4a</i> [^] SS cluster_208995		2,743	5,795	1.08	0.97	N.D.	
Vv- <i>TAS4c</i> [^] SS cluster_2480		1	83	6.37	0.03	N.D.	
Vv- <i>TAS4b</i> [^] SS cluster_208942	694.7	181	474	1.39	0.51	N.D.	
MYBA7, D4(-) tarVIT_14s0006g01280		N.D.	N.D.			N.D.	
MYBA6, D4(-) tarVIT_14s0006g01290	38.1	N.D.	N.D.		0.43	N.D.	
vvi- <i>MIR828</i> , SS cluster_242339		N.D.	N.D.			2.52	0.05
MYB-828 target\$ VIT_14s0066g01220	333.0	0	0.9	-0.8	0.008	-1.19	0.11
MYB-828 target\$ VIT_00s0341g00050		2	3	0.59	0.50	0.005	0.10
MYB-828 target\$ VIT_09s0002g01380	568.4	4	11	1.45	0.03	1.76	0.09
MYB-828 target\$ VIT_17s0000g08480	206.4	0	17	-5		N.D.	
MYB;clust_49088VIT_04s0079g00410	24.6	1	1.4	0.50	0.45	1.54	0.006
vvi- <i>MIR403a</i> ;c		N.D.	N.D.			1.9; 2.24	0.07
vvi- <i>MIR403f</i> , SS cluster_95226		107	151	0.50	0.10	0.69	0.18
AGO2;mir403 tarVIT_10s0042g01180	50.0	2	7.1	1.82	0.12	-0.09	0.10
vvi- <i>MIR827</i> , SS cluster_75145		204	152	-0.43	0.83	N.D.	
vvi- <i>MIR5645bL</i> ;clust_306046;assocSPX	9.1	0	0.7	-0.5	0.45	N.D.	
MFS; SPX targetVIT_02s0025g04540	71.1	1	9.2	3.20	0.38	1.59	0.01
MFS; SPX targetVIT_17s0000g05460	183.4	22	32.1	0.55	0.91	-0.02	0.11
vvi- <i>MIR399ig</i> , SS clust_19628/140078		8	10.2	0.36	0.70	N.D.	
VvPHT2;1,mir399assoc00s0291g00060		N.D.	N.D.			-1.34	0.02
VvPHT1;4L,mir399assoc05s0049g00930		N.D.	N.D.			-1.1	0.09
VvPHT1;4L,mir399assoc07s0005g03290		N.D.	N.D.			-1.06	0.05
VvPHT1;4L,mir399assoc07s0005g03300		N.D.	N.D.			0.92	0.20
TAS2candVIT_14s0030g02280.targPPR	423.3	3	34.2	3.51	0.007	-0.26	0.32
DCL2; VIT_04s0023g00920	33.8	1	2.5	1.30	0.09	-0.70	0.03
SGS3; VIT_07s0130g00190	177.4	15	30.4	1.02	0.28	-0.53	0.03

* ShortStack (SS)¹⁵ output, 28 libraries. phasiRNA/miRNAs normalized to reads per 2 mill. ND: not detected

¶ False Discovery Rate < 0.1; Benjamini & Hochberg multiple comparisons adjustment.

\$ validated class1, degradome: 5,669 reads; 6,823 reads; 1,200 reads ; 5,540 reads, respectively²⁰.

‡, † log₂-Fold Change stats calculated by DESeq2^{19, 44} or kallisto/sleuth⁴⁵, respectively.

[^] phytozome.jgi.doe.gov genome coordinates from Rock²¹. Vv-*TAS4a* maps to VIT_14s0006g03100.

AtPHT2;1 is strongly up-regulated by infection with the gram-negative, phloem-limited bacterium *Candidatus Liberibacter* associated with ~30 fold increased *csi-miR399* expression that targets *PHO2*². Consistent with prior findings, we also observe up-regulation of vvi-*miR399ig* and mis-regulation of downstream *PHT1;4L* family members by XF (Table III), supporting the notion that phosphate homeostasis is key to XF disease etiology via phosphate-regulated miR828, 827, and 399. Altered activity of miR827 in response to XF predicts that its target *SPX1* would decrease while SPX ligand MFS would be relieved of SPX repression; we observed significant up-regulation of MFS (Table III), **strongly supporting the hypothesized molecular mechanism**. Concordant (instead of canonical predicted inverse) changes in P₁-inducible miRNAs and their targets (Table III) has been observed in rice⁴¹ and Arabidopsis¹, supporting a modified model that not only miR828, but also miR827 and

miR399 circuits are under complex regulation (e.g. autoregulation). We also have evidence of such complex regulation by virtue of MFS loci generating abundant phasiRNAs (Table III). The post-transcriptional silencing effector *AGO2* is also a phasi-producing locus targeted by miR403⁴⁶, which we find is significantly up-regulated by XF infection at the expense of *AGO2*, consistent with the RNAi model. We also confirm in grape the finding in soybean^{47, 48} that miRNA biogenesis effector *DCL2* is subject to PTGS resulting in phasiRNA accumulation (Table III).

Many of those top-listed significantly differentially regulated *PHAS* and *TAS* genes discovered by PhaseTank and ShortStack are known effectors of plant pathogen responses (Leucine-Rich-Repeat receptors, Pentatricopeptide Repeat proteins) mediated by miRNA activities^{13, 14}. Over 150 LRRs out of the 341 such genes annotated in grapevine⁴⁹ are differentially regulated by XF infection in our mRNA-Seq, sRNA, and degradome datasets. The results to date show these loci produce phasiRNAs (high) in inverse proportion to their target mRNA abundances (low; data not shown). Such clustering of gene ontology for disease resistance loci in our RNA-Seq, sRNA, and degradome datasets **very strongly support the working model** that XF infection modulates phasiRNA production in loci other than MIR828/TAS4 known to control pathogen resistance.

Summary of accomplishments and results, Objective II. The working model for PD etiology by altered phosphate regulation of miR828/*TAS4* and *MYB* target genes is supported by our sRNA and RNA-Seq datasets. A highly correlated network of miRNA/phased siRNA-producing- and *TAS* noncoding loci known to function in plant immunity across plant taxa is observed. A transgenic tobacco model shows that XF infection modulates the *TAS4* autoregulatory loop, which correlates with PD symptom severity. A direct test of the model in grapevine (and tobacco, Objective I) by genome editing of the positive and negative effector loci is well grounded now, based on our deep sequencing evidence for miR828/*TAS4* roles in PD.

III. Characterize the changes in (a) xylem sap and leaf Pi, and (b) polyphenolic levels of XF-infected canes and leaves. (c) Test on tobacco in the greenhouse and XF growth in vitro the P_i analogue phosphite as a durable, affordable and environmentally sound protectant/safener for PD.

(a) Leaf [Pi]. In the last progress report (Oct. 2016) we showed a significantly different (unexpectedly higher) concentration of Pi in XF-infected canes, internally controlled for sulfate and nitrate concentrations. This intriguing result warrants further study, but we have yet to follow up due to lack of samples. A field trip is planned for May 2017. We have petiole samples from each independent cane assayed in 2016, so we are assaying XF titers in subtending leaf petioles to directly correlate with Pi results from cane xylem sap. Jun-Yi Yang's group showed that overexpression in Arabidopsis of Secreted Aster Yellow's phytoplasma strain Witches' Broom Protein11 (SAP11) suppresses plant defense responses by triggering accumulation of cellular P_i. This is the same observation we reported for xylem sap in the last progress report. This result is consistent with observed increased expression of P_i starvation-induced miR827 and miR5645⁵⁰ (Table III). Our working hypothesis based on available evidence is that XF causes an imbalance of Pi between leaf (hypothesized low) and xylem (observed high) caused by XF infection.

(b) Polyphenolics in XF-infected canes and leaves. Analyses of xylem sap anthocyanin and XF titers from petiole extracts are ongoing by tandem MS|MS fragmentation monitoring for fragment ion(s) representing malvin and cyanin aglycone species.

(c) P_i analogue phosphite as effector of XF growth and safener of disease symptoms. The Cooperator (De La Fuente) will ship XF Temecula-1 and WM-1 strains to the PI. No progress has been made since the last report on this Objective due to high priority efforts on Objective II. Future work will focus first on assessing phosphite effects on XF growth rates in liquid culture. If results are positive, safener treatments of tobacco and grapevine under greenhouse XF challenge will follow.

Summary of accomplishments and results, Objective III. Together with MIRNA genes and target effectors of phosphate homeostasis revealed from Objective II, we have direct evidence for xylem sap inorganic phosphate (Pi) involvement in PD that further substantiates the working hypothesis.

PUBLICATIONS PRODUCED AND PENDING, PRESENTATIONS

Rock, C.D. (2017) "Phenylpropanoid metabolism." Invited review, in press. *Encyclopedia of Life Science*. Chichester, UK: John Wiley and Sons. www.els.net.

Sunitha S, Traore S, Azad Md.F, De La Fuente L, Rock C. Poster #1000-063. "Conservation of an autoregulatory feedback loop regulating anthocyanin biosynthesis in dicots." Plant Biology 2016: Annual Meeting of the American Society of Plant Biologists. July 9-13, 2016. Austin, TX.

Talk and poster on this project. CDFFA-PD/GWSS Symposium 2016. San Diego CA, Dec. 12-13, 2016.

RESEARCH RELEVANCE STATEMENT

The PD-GWSS Board has suggested knocking out genes involved in diffusible signals and host chemical specificity for PD etiology by CRISPR/Cas9. This project endeavors to meet that mandate.

LAYPERSON SUMMARY OF PROJECT ACCOMPLISHMENTS

Our proof-in-principle experimental results to date are impacting understanding host-vector-pathogen interactions in PD. We have generated strong evidence from our mRNA-Seq, sRNA-Seq and degradome datasets from XF-infected grape and tobacco materials, quantitation of xylem sap phosphate in PD-infected canes, and disease severity correlations with molecular phenotypes from greenhouse XF challenge experiments that support a refined model that XF is using host small RNAs as a 'trojan horse' that could serve as a paradigm to understand not only phosphate as diffusible signal for synthesis of host polyphenolic anti-bacterial metabolites in PD etiology, but also the pleiotropic traits of "green islands" and "matchstick petioles," among others.

STATUS OF FUNDS

Salaries funds have been fully encumbered for postdoctoral fellow Dr. Sunitha; the balance of ~\$7,000 will be encumbered to cover the 2017 summer session for two graduate students; Fakhru Azad, working on phosphate and anthocyanins, and another TBA. Major consumables expenses have been committed to purchase more Illumina sequencing by IIGB/UC Riverside (~\$8,000) and Illumina TruSeq mRNA stranded- and smallRNA library kits (~\$8,000) for samples to be collected and processed from the field this spring. Travel funds will be spent on two or more field trips to CA to collect xylem sap in May/June, and PD tissue samples in July/August.

SUMMARY AND STATUS OF INTELLECTUAL PROPERTY ASSOCIATED WITH PROJECT

The PI's USPTO patent application #13/874,962 received a USPTO first office action May 18, 2016 to reject claims (Section 101 grounds; cf. SCOTUS 2013 *Myriad Genetics* case on genes as non-patentable matter occurring in nature). The TTU Office of Technology Commercialization filed on behalf of the PI a response on October 18, 2016; we await the Examiner's response. The PI will pursue patent protection because genome editing rises above the standard set by Section 101 that naturally occurring genes cannot be patented. It was anticipated there would be such a USPTO rejection of claims, as the claims were originally written based on the PI's publication¹² that taught there are broad applications and potential for engineering the subject genes, when the invention had yet to be enabled.

LITERATURE CITED

1. Hsieh LC, Lin SI, Shih ACC, Chen JW, Lin WY, Tseng CY, Li WH, Chiou TJ. (2009) **Uncovering small RNA-mediated responses to phosphate deficiency in Arabidopsis by deep sequencing.** *Plant Physiol* **151**: 2120-2132
2. Zhao H, Sun R, Albrecht U, Padmanabhan C, Wang A, Coffey MD, Girke T, Wang Z, Close TJ, Roose M, Yokomi RK, Folimonova S, Vidalakis G, Rouse R *et al.* (2013) **Small RNA profiling reveals phosphorus deficiency as a contributing factor in symptom expression for citrus Huanglongbing disease.** *Mol Plant* **6**: 301-310
3. Jacobs T, LaFayette P, Schmitz R, Parrott W. (2015) **Targeted genome modifications in soybean with CRISPR/Cas9.** *BMC Biotechnol* **15**: 16
4. Mali P, Yang L, Esvelt KM, Aach J, Guell M, DiCarlo JE, Norville JE, Church GM. (2013) **RNA-guided human genome engineering via Cas9.** *Science* **339**: 823-826
5. De La Fuente L, Parker JK, Oliver JE, Granger S, Brannen PM, van Santen E, Cobine PA. (2013) **The bacterial pathogen *Xylella fastidiosa* affects the leaf ionome of plant hosts during infection.** *PLoS ONE* **8**: e62945
6. Velten J, Cakir C, Youn E, Chen J, Cazzonelli CI. (2012) **Transgene silencing and transgene-derived siRNA production in tobacco plants homozygous for an introduced *AtMYB90* construct.** *PLoS ONE* **7**: e30141
7. Zhu X, Xu Y, Yu S, Lu L, Ding M, Cheng J, Song G, Gao X, Yao L, Fan D, Meng S, Zhang X, Hu S, Tian Y. (2014) **An efficient genotyping method for genome-modified animals and human cells generated with CRISPR/Cas9 system.** *Sci Rep* **4**: 6420
8. Wu X, Kriz AJ, Sharp PA. (2014) **Target specificity of the CRISPR-Cas9 system.** *Quant Biol* **2**: 59-70
9. Aukerman MJ, Hirschfeld M, Wester L, Weaver M, Clack T, Amasino RM, Sharrock RA. (1997) **A deletion in the *PHYD* gene of the Arabidopsis Wassilewskija ecotype defines a role for phytochrome D in red/far-red light sensing.** *Plant Cell* **9**: 1317-1326
10. Usadel B, Poree F, Nagel A, Lohse M, Czedik-Eysenberg A, Stitt M. (2009) **A guide to using MapMan to visualize and compare Omics data in plants: a case study in the crop species, maize.** *Plant Cell Environ* **32**: 1211-1229
11. Thimm O, Bläsing O, Gibon Y, Nagel A, Meyer S, Kruger P, Selbig J, Muller LA, Rhee SY, Stitt M. (2004) **MAPMAN: a user-driven tool to display genomics data sets onto diagrams of metabolic pathways and other biological processes.** *Plant J* **37**:
12. Luo Q-J, Mittal A, Jia F, Rock CD. (2012) **An autoregulatory feedback loop involving *PAP1* and *TAS4* in response to sugars in Arabidopsis.** *Plant Mol Biol* **80**: 117-129
13. Addo-Quaye C, Eshoo TW, Bartel DP, Axtell MJ. (2008) **Endogenous siRNA and miRNA targets identified by sequencing of the Arabidopsis degradome.** *Curr Biol* **18**: 758-762
14. German MA, Pillay M, Jeong DH, Hetawal A, Luo SJ, Janardhanan P, Kannan V, Rymarquis LA, Nobuta K, German R, De Paoli E, Lu C, Schroth G, Meyers BC *et al.* (2008) **Global identification of microRNA-target RNA pairs by parallel analysis of RNA ends.** *Nat Biotech* **26**: 941-946
15. Johnson NR, Yeoh JM, Coruh C, Axtell MJ. (2016) **Improved placement of multi-mapping small RNAs.** *G3: Genes/Genomes/Genetics* **6**: 2103-2111
16. Guo QL, Qu XF, Jin WB. (2015) **PhaseTank: genome-wide computational identification of phasiRNAs and their regulatory cascades.** *Bioinformatics* **31**: 284-286
17. Rogers EE. (2012) **Evaluation of Arabidopsis thaliana as a model host for Xylella fastidiosa.** *Mol Plant-Microbe Interact* **25**: 747-754
18. Thieme CJ, Rojas-Triana M, Stecyk E, Schudoma C, Zhang W, Yang L, Miñambres M, Walther D, Schulze WX, Paz-Ares J, Scheible W-R, Kragler F. (2015) **Endogenous Arabidopsis messenger RNAs transported to distant tissues.** *Nat Plants* **1**: 15025
19. Anders S, Huber W. (2010) **Differential expression analysis for sequence count data.** *Genome Biol* **11**: R106
20. Pantaleo V, Szittyta G, Moxon S, Miozzi L, Moulton V, Dalmay T, Burgyan J. (2010) **Identification of grapevine microRNAs and their targets using high-throughput sequencing and degradome analysis.** *Plant J* **62**: 960-976
21. Rock CD. (2013) **Trans-acting small interfering RNA4: key to nutraceutical synthesis in grape development?** *Trends Plant Sci* **18**: 601-610

22. Song X, Li P, Zhai J, Zhou M, Ma L, Liu B, Jeong D-H, Nakano M, Cao S, Liu C, Chu C, Wang X-J, Green PJ, Meyers BC *et al.* (2012) **Roles of DCL4 and DCL3b in rice phased small RNA biogenesis.** *Plant J* **69**: 462-474
23. Vogel JP, Garvin DF, Mockler TC, Schmutz J, Rokhsar D, Bevan MW, Barry K, Lucas S, Harmon-Smith M, Lail K, Tice H, Grimwood J, McKenzie N, Huo NX *et al.* (2010) **Genome sequencing and analysis of the model grass *Brachypodium distachyon*.** *Nature* **463**: 763-768
24. Shivaprasad PV, Chen HM, Patel K, Bond DM, Santos B, Baulcombe DC. (2012) **A microRNA superfamily regulates nucleotide binding site-leucine-rich repeats and other mRNAs.** *Plant Cell* **24**: 859-874
25. Johnson C, Kasprzewska A, Tennessen K, Fernandes J, Nan GL, Walbot V, Sundaresan V, Vance V, Bowman LH. (2009) **Clusters and superclusters of phased small RNAs in the developing inflorescence of rice.** *Genome Res* **19**: 1429-1440
26. Klevebring D, Street N, Fahlgren N, Kasschau K, Carrington J, Lundeberg J, Jansson S. (2009) **Genome-wide profiling of *Populus* small RNAs.** *BMC Genomics* **10**: 620
27. Lin J-S, Lin C-C, Lin H-H, Chen Y-C, Jeng S-T. (2012) **MicroR828 regulates lignin and H₂O₂ accumulation in sweet potato on wounding.** *New Phytol* **196**: 427-440
28. Xia R, Zhu H, An Y-q, Beers E, Liu Z. (2012) **Apple miRNAs and tasiRNAs with novel regulatory networks.** *Genome Biol* **13**: R47
29. Zhu H, Xia R, Zhao BY, An YQ, Dardick CD, Callahan AM, Liu ZR. (2012) **Unique expression, processing regulation, and regulatory network of peach (*Prunus persica*) miRNAs.** *BMC Plant Biol* **12**: 18
30. Zhai J, Jeong D-H, De Paoli E, Park S, Rosen BD, Li Y, Gonzalez AJ, Yan Z, Kitto SL, Grusak MA, Jackson SA, Stacey G, Cook DR, Green PJ *et al.* (2011) **MicroRNAs as master regulators of the plant NB-LRR defense gene family via the production of phased, *trans*-acting siRNAs.** *Genes Dev* **25**: 2540-2553
31. Zhang C, Li G, Wang J, Fang J. (2012) **Identification of *trans*-acting siRNAs and their regulatory cascades in grapevine.** *Bioinformatics* **28**: 2561-2568
32. Guan X, Pang M, Nah G, Shi X, Ye W, Stelly DM, Chen ZJ. (2014) **miR828 and miR858 regulate homoeologous MYB2 gene functions in Arabidopsis trichome and cotton fibre development.** *Nat Commun* **5**: 3050
33. Källman T, Chen J, Gyllenstrand N, Lagercrantz U. (2013) **A significant fraction of 21 nt sRNA originates from phased degradation of resistance genes in several perennial species.** *Plant Physiol* **162**: 741-754
34. Xia R, Xu J, Arikiti S, Meyers BC. (2015) **Extensive families of miRNAs and PHAS loci in Norway spruce demonstrate the origins of complex phasiRNA networks in seed plants.** *Mol Biol Evol* **32**: 2905-2918
35. Turner M, Yu O, Subramanian S. (2012) **Genome organization and characteristics of soybean microRNAs.** *BMC Genomics* **13**: 169
36. Xia R, Meyers BC, Liu Z, Beers EP, Ye S, Liu Z. (2013) **MicroRNA superfamilies descended from miR390 and their roles in secondary small interfering RNA biogenesis in Eudicots.** *Plant Cell* **25**: 1555-1572
37. Li F, Pignatta D, Bendix C, Brunkard JO, Cohn MM, Tung J, Sun H, Kumar P, Baker B. (2012) **MicroRNA regulation of plant innate immune receptors.** *Proc Natl Acad Sci U S A* **109**: 1790-1795
38. Choi H-K, Iandolino A, da Silva FG, Cook DR. (2013) **Water deficit modulates the response of *Vitis vinifera* to the Pierce's disease pathogen *Xylella fastidiosa*.** *Mol Plant-Microbe Interact* **26**: 643-657
39. Lin W-Y, Huang T-K, Chiou T-J. (2013) **NITROGEN LIMITATION ADAPTATION, a target of microRNA827, mediates degradation of plasma membrane-localized phosphate transporters to maintain phosphate homeostasis in Arabidopsis.** *Plant Cell* **25**: 4061-4074
40. Fahlgren N, Howell MD, Kasschau KD, Chapman EJ, Sullivan CM, Carrington JC. (2007) **High-throughput sequencing of Arabidopsis microRNAs: evidence for frequent birth and death of MIRNA genes.** *PLoS ONE* **2**: e219
41. Lin S-I, Santi C, Jobet E, Lacut E, El Kholti N, Karlowski WM, Verdeil J-L, Breitler JC, Périn C, Ko S-S, Guiderdoni E, Chiou T-J, Echeverria M. (2010) **Complex regulation of two target genes encoding SPX-MFS proteins by rice miR827 in response to phosphate starvation.** *Plant Cell Physiol* **51**: 2119-2131

42. Park BS, Seo JS, Chua N-H. (2014) **NITROGEN LIMITATION ADAPTATION recruits PHOSPHATE2 to target the phosphate transporter PT2 for degradation during the regulation of Arabidopsis phosphate homeostasis.** *Plant Cell* **26**: 454-464
43. Hackenberg M, Shi B-J, Gustafson P, Langridge P. (2013) **Characterization of phosphorus-regulated miR399 and miR827 and their isomirs in barley under phosphorus-sufficient and phosphorus-deficient conditions.** *BMC Plant Biol* **13**: 214
44. Love MI, Huber W, Anders S. (2014) **Moderated estimation of fold change and dispersion for RNA-seq data with DESeq2.** *Genome Biol* **15**: 550
45. Pimentel HJ, Bray N, Puente S, Melsted P, Pachter L. (2016) **Differential analysis of RNA-Seq incorporating quantification uncertainty.** *bioRxiv*: 10.1101/058164
46. Zhang C, Xian Z, Huang W, Li Z. (2015) **Evidence for the biological function of miR403 in tomato development.** *Sci Hort* **197**: 619-626
47. Zhao MX, Cai CM, Zhai JX, Lin F, Li LH, Shreve J, Thimmapuram J, Hughes TJ, Meyers BC, Ma JX. (2015) **Coordination of microRNAs, phasiRNAs, and NB-LRR genes in response to a plant pathogen: insights from analyses of a set of soybean *Rps* gene near-isogenic lines.** *Plant Genome* **8**: doi: 10.3835/plantgenome2014.3809.0044
48. Zhao MX, Meyers BC, Cai CM, Xu W, Ma JX. (2015) **Evolutionary patterns and coevolutionary consequences of *MIRNA* genes and microRNA targets triggered by multiple mechanisms of genomic duplications in soybean.** *Plant Cell* **27**: 546-562
49. Di Gaspero G, Cipriani G, Adam-Blondon AF, Testolin R. (2007) **Linkage maps of grapevine displaying the chromosomal locations of 420 microsatellite markers and 82 markers for R-gene candidates.** *Theor Appl Genet* **114**: 1249-1263
50. Lu Y-T, Li M-Y, Cheng K-T, Tan CM, Su L-W, Lin W-Y, Shih H-T, Chiou T-J, Yang J-Y. (2014) **Transgenic plants that express the phytoplasma effector SAP11 show altered phosphate starvation and defense responses.** *Plant Physiol* **164**: 1456-1469